ISSN 1674-1056
http://cpb.iphy.ac.cn
http://iopscience.iop.org/cpb
中国物理 B
Chinese Physics
中国物理 Chinese Physics B

Synthesis and thermoelectric properties of Nd-single filled p-type skutterudites

Hong Wu(吴宏), Nusrat Shaheen, Heng-Quan Yan(杨恒全), Kun-Ling Peng(彭坤岭), Xing-Chen Shen(沈星辰), Guo-Yu Wang(王国玉), Xu Lu(卢旭), Xiao-Yuan Zhou(周小元)
Citation: Chin. Phys. B . 2018, 27(4): 047203. **doi:** 10.1088/1674-1056/27/4/047203

Journal homepage: http://cpb.iphy.ac.cn; http://iopscience.iop.org/cpb

What follows is a list of articles you may be interested in

Multinary diamond-like chalcogenides for promising thermoelectric application

Dan Zhang(张旦), Hong-Chang Bai(白洪昌), Zhi-Liang Li(李志亮), Jiang-Long Wang(王江龙), Guang-Sheng Fu(傅广生), Shu-Fang Wang(王淑芳)
Chin. Phys. B . 2018, 27(4): 047206. **doi:** 10.1088/1674-1056/27/4/047206

Band engineering and precipitation enhance thermoelectric performance of SnTe with Zn-doping

Zhiyu Chen(陈志禹), Ruifeng Wang(王瑞峰), Guoyu Wang(王国玉), Xiaoyuan Zhou(周小元), Zhengshang Wang(王正上), Cong Yin(尹聪), Qing Hu(胡庆), Binqiang Zhou(周斌强), Jun Tang(唐军), Ran Ang(昂然)
Chin. Phys. B . 2018, 27(4): 047202. **doi:** 10.1088/1674-1056/27/4/047202

Biaxial strain-induced enhancement in the thermoelectric performance of monolayer WSe_2

Wanhuizi Shen(沈婉慧子), Daifeng Zou(邹代峰), Guozheng Nie(聂国政), Ying Xu(许英)
Chin. Phys. B . 2017, 26(11): 117202. **doi:** 10.1088/1674-1056/26/11/117202

Optimize the thermoelectric performance of CdO ceramics by doping Zn

Xin-Yu Zha(查欣雨), Lin-Jie Gao(高琳洁), Hong-Chang Bai(白洪昌), Jiang-Long Wang(王江龙), Shu-Fang Wang(王淑芳)
Chin. Phys. B . 2017, 26(10): 107202. **doi:** 10.1088/1674-1056/26/10/107202

Thermoelectric properties of Li-doped $Sr_{0.7}Ba_{0.3}Nb_2O_{6-\delta}$ ceramics

Ya-Cui Zhang(张亚翠), Jian Liu(刘剑), Yi Li(李宜), Yu-Fei Chen(陈宇飞), Ji-Chao Li(李吉超), Wen-Bin Su(苏文斌), Yu-Cheng Zhou(周昱成), Jin-Ze Zhai(翟近泽), Teng Wang(王腾), Chun-Lei Wang(王春雷)
Chin. Phys. B . 2017, 26(10): 107201. **doi:** 10.1088/1674-1056/26/10/107201

SPECIAL TOPIC — Recent advances in thermoelectric materials and devices

Synthesis and thermoelectric properties of Nd-single filled p-type skutterudites*

Hong Wu(吴宏)[1,2], Nusrat Shaheen[1], Heng-Quan Yang(杨恒全)[1], Kun-Ling Peng(彭坤岭)[1,2], Xing-Chen Shen(沈星辰)[1,2], Guo-Yu Wang(王国玉)[2], Xu Lu(卢旭)[1], and Xiao-Yuan Zhou(周小元)[1,†]

[1] *Department of Applied Physics, Chongqing University, Chongqing* 400044, *China*
[2] *Chongqing Institute of Green and Intelligent Technology, Chinese Academy of Sciences, Chongqing* 400714, *China*

(Received 2 September 2017; revised manuscript received 5 October 2017; published online 10 March 2018)

We report the synthesis of Nd-filled and Fe substituted p-type $Nd_xFe_{3.2}Co_{0.8}Sb_{12}$ ($x = 0.5$, 0.6, 0.7, 0.8, and 0.9) skutterudites by the solid-state reaction method. The influences of Nd filler on the electrical and thermal transport properties are investigated in a temperature range from room temperature to 850 K. A lowest lattice thermal conductivity of 0.88 $W{\cdot}m^{-1}{\cdot}K^{-1}$ is obtained in $Nd_{0.8}Fe_{3.2}Co_{0.8}Sb_{12}$ at 673 K, which results from the localized vibration modes of fillers and the increase of grains boundaries. Meanwhile, the maximum power factor is 2.77 $mW{\cdot}m^{-1}{\cdot}K^{-2}$ for the $Nd_{0.9}Fe_{3.2}Co_{0.8}Sb_{12}$ sample at 668 K. Overall, the highest dimensionless figure of merit $zT = 0.87$ is achieved at 714 K for $Nd_{0.9}Fe_{3.2}Co_{0.8}Sb_{12}$.

Keywords: thermoelectric, p-type skutterudites, neodymium filler, lattice thermal conductivity

PACS: 72.15.Jf. 74.25.fg, 74.25.fc, 74.25.F– **DOI:** 10.1088/1674-1056/27/4/047203

1. Introduction

A great deal of effort has been devoted to developing highly efficient thermoelectric (TE) materials, which can convert waste heat into useful electricity.[1] The thermoelectric performance of a material is evaluated by the dimensionless figure of merit ($zT = S^2T\sigma\kappa^{-1}$), where S, T, σ, and κ are the Seebeck coefficient, absolute temperature, electrical conductivity, and thermal conductivity, respectively.[2] The skutterudites based thermoelectric materials are of particular interest since they possess high thermoelectric performance, good thermal stability and excellent mechanical properties. They are therefore considered as a promising candidate for waste heat recovery for automobiles. The thermoelectric performance of pure skutterudite is limited by its rather high thermal conductivity, primarily the lattice part.[3] The skutterudite is represented as a general formula MX_3 with a body centered cubic phase structure, where M (e.g., Co, Rh, and Fe) refers to the transition metal and X represents the pnictogen atom (e.g., As, P, and Sb). There are two voids per unit cell with sufficient size, which can be easily accommodated with other metal atoms, then the general formula for the compound becomes RM_4X_{12}, where R is the filler metal atom, which is weakly bounded with the surrounding atoms in the matrix.[4] Slack *et al.* proposed that the lattice thermal conductivity could be greatly reduced when the filler atoms are located in the voids of skutterudites, which is due to the strong phonon scattering caused by localized vibration modes of filler atoms.[5,6] In the last decade, the strategies for reducing the thermal conductivity of skutterudites have involved the manipulation of filling atoms with the different types of fraction modes and vibration modes.[7]

However, most of the work has focused on the n-type skutterudites, which shows high zT values over 1.7.[8] The highest zT value of the p-type skutterudite is much lower than that of the n-type one. From a practical point of view, both n-type and p-type are equally important for power generation devices. Up to now, enhancing the thermoelectric performance of the p-type skutterudites has been a challenging task. Typically, the p-type skutterudite can be attained by the partial substitution of Fe for Co in a pure $CoSb_3$ skutterudite compound, where Fe atoms have less valence electrons than Co atoms. Usually, the Fe-to-Co ratio can be tuned on the transition metal site together with void filling, while the Seebeck coefficient can be enlarged by pushing the Fermi level into the heavier transition metal d-bands. However, the large effective mass of holes in skutterudite and stronger alloy scattering after Fe substitution deteriorate the carrier mobility significantly, thereby causing a diminished power factor, which is about half the value of the corresponding n-type skutterudite. In addition, the bipolar conduction caused by electron-hole pairs moving across the band gap at high temperatures leads to a higher ther-

*Project supported by the National Natural Science Foundation of China (Grant Nos. 11674040, 11404044, 51472036, 51672270, and 51401202), the Fundamental Research Funds for the Central Universities (Grant No. 106112016CDJZR308808), the 100 Talent Program of the Chinese Academy of Sciences (Grant No. 2013-46), and the Project for Fundamental and Frontier Research in Chongqing, China (Grant No. CSTC2015JCYJBX0026).

†Corresponding author. E-mail: xiaoyuan2013@cqu.edu.cn

© 2018 Chinese Physical Society and IOP Publishing Ltd

mal conductivity. These factors are hindering improvement to the thermoelectric performance in p-type skutterudite.[9]

Many researchers have tried to fill the voids with different rattlers. Tang *et al.* reported that the single phase barium-filled p-type skutterudite compound and achieved a zT value of 0.9 at 750 K in $Ba_{0.27}Fe_{0.98}Co_{3.02}Sb_{12}$.[10] Tan *et al.* studied the Ce-filled p-type skutterudites and achieved the highest zT value of 1.0 at 800 K in $Ce_{1.1}Fe_4Sb_{12}$.[12] Zhu *et al.* investigated the double filled Yb–La and attained the highest zT value of 1.0 at 700 K in $Yb_{0.25}La_{0.60}Fe_{2.7}Co_{1.3}Sb_{12}$.[13,14] Herein, we report the systematic study on the thermoelectric performance of Nd-filled p-type skutterudites with compositions of $Nd_xFe_{3.2}Co_{0.8}Sb_{12}$ ($x = 0.5$, 0.6, 0.7, 0.8, and 0.9) synthesized by the traditional method of melting-annealing and further followed by a spark plasma sintering process. It is observed that the electrical conductivity decreases while the Seebeck coefficient increases with increasing the Nd filling fraction. The thermal conductivity is reduced by the Nd fillers through the rattling effect along with the nanostructured precipitate through strengthened phonon scattering. A maximum zT value of 0.87 is achieved for $Nd_{0.9}Fe_{3.2}Co_{0.8}Sb_{12}$ at 714 K due to its high power factor and low thermal conductivity.

2. Experimental details

Nd-filled p-type skutterudites with compositions of $Nd_xFe_{3.2}Co_{0.8}Sb_{12}$ ($x = 0.5$, 0.6, 0.7, 0.8, and 0.9) were synthesized by the solid-state reaction method. In a typical process, high-purity elemental materials of Nd (ingot 99.99%), Fe (pieces 99.99 %), Co (slugs and foils 99.99%), and Sb (chunk 99.99%) were mixed according to the stoichiometric ratios and placed in carbon coated quartz tubes inside a glove box. The sealed quarts tubes were heated up to 1373 K with a ramp rate of 3 K·min^{-1}, maintained for 27 h and then quenched in saturated salt water. The resulting chunks were ground into powder samples and they were cold-pressed into cylinders with a diameter of 10 mm. These cylinders were sealed in tubes again for further annealing at 923 K for 7 days. The annealed ingots were ground into fine powders and loaded into graphite dies with an inner-diameter of 10 mm for spark plasma sintering (SPS-625) at 833 K for 11 min under a pressure of 45 MPa. The sintered samples were cut and polished into bars (2 mm×3 mm×10 mm) for electrical transport property measurement and disks (10 mm in diameter and 2 mm in thickness) for thermal conductivity measurement, respectively.

The phase structures and purities of the as-annealed ingots were characterized by a powder x-ray diffraction (XRD) apparatus (PANalytical X'pert powder with Cu Kα radiations). The morphologies and homogeneities of the samples were investigated by the field emission scanning electron microscopy (JSM-7800F, JEOL). The electrical conductivity and Seebeck coefficient were measured by the static direct-current method using a commercial equipment LSR-3. The total thermal conductivities of the samples ranging from 300 K–850 K were calculated from the relationship $\kappa = \lambda C_p d$, where λ is the thermal diffusivity measured using the laser flash method (LFA 457) and C_p is the specific heat measured using the Netzsch 404 F3. The densities of the samples were obtained using the Archimedes method, and relative densities are higher than 95% of the theoretical value. Room temperature carrier concentration was determined using a home-made Hall measurement system with the magnetic field of ± 1 T.

3. Results and discussion

The XRD patterns of the $Nd_xFe_{3.2}Co_{0.8}Sb_{12}$ ($x = 0.5$, 0.6, 0.7, 0.8, and 0.9) are presented in Fig. 1(a). All the peaks are well matched with the standard reference data of the JCPDF-65-8978 card with skutterudites phase except that a trace of Sb impurity phase is found at $x = 0.9$. All samples remain in the body centered cubic structure with the space group of *Im*-3. In addition, the lattice parameters for each sample are shown in Fig. 1(b). The lattice parameter slightly increases with filler (Nd) content increasing (see Fig. 1(b)), which can enlarge the icosahedron in the unit cell.

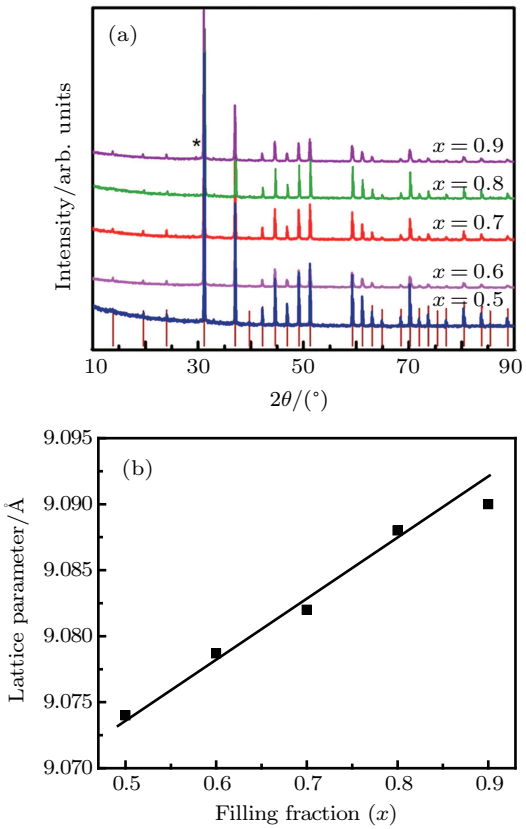


Fig. 1. (color online) (a) XRD patterns and (b) lattice parameters of $Nd_xFe_{3.2}Co_{0.8}Sb_{12}$ ($x = 0.5$, 0.6, 0.7, 0.8, and 0.9) as-sintered samples.

The SEM images of the as-sintered bulk of $Nd_{0.9}Fe_{3.2}Co_{0.8}Sb_{12}$ sample are shown in Fig. 2. From the

SEM images, we observe that the crystallized grains are closely packed, which indicates the high density of bulk material. The majority of the grain sizes range from hundreds of nanometers to a few micrometers. Also, there exist many nanoparticles in the matrix as shown in Fig. 2(b). The non-uniform distribution in grain sizes and nanoparticles can help to scatter phonons with different mean free paths. Also, the tight junction feature of crystallized grains is beneficial to charge carrier transportation.

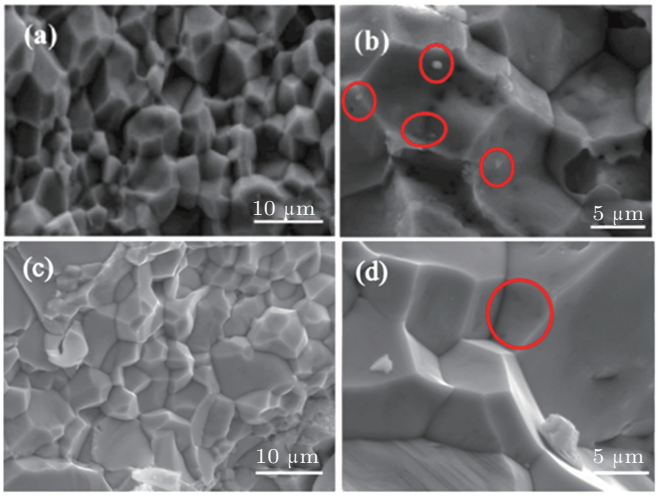


Fig. 2. (color online) [(a) and (b)] SEM images of $Nd_{0.9}Fe_{3.2}Co_{0.8}Sb_{12}$ and [(c) and (d)] $Nd_{0.7}Fe_{3.2}Co_{0.8}Sb_{12}$ as-sintered sample with different resolutions.

The temperature-dependent electrical properties of the $Nd_xFe_{3.2}Co_{0.8}Sb_{12}$ ($x = 0.5$, 0.6, 0.7, 0.8, and 0.9) filled skutterudites are displayed in Fig. 3(a). With increasing Nd concentration, the electrical conductivity decreases due to the reduction in the carrier concentration, i.e., the carrier concentration for the $x = 0.5$ sample is 5.5×10^{20} cm^{-3}, which is reduced to 3.5×10^{20} cm^{-3} for the $x = 0.9$ sample as listed in Table 1. The carrier concentration decreases with increasing Nd content because the electrons are donated from the filler atoms. The $Nd_{0.5}Fe_{3.2}Co_{0.8}Sb_{12}$ sample shows a typical highly-degenerate semiconductor behavior, where the electrical conductivity gradually decreases with increasing temperature over the whole temperature range. However, the other samples show an increase trend in electrical conductivity at high temperatures (> 700 K), which may be attributed to the bipolar effect. Generally, with increasing temperature, the electrical conductivity decreases, which is attributed to stronger electron scattering at higher temperatures. Also with further increasing temperature, the decrease in electrical conductivity is comparatively slow. This is probably due to the gradually increased carrier concentration from thermal excitation or the variation in the carrier scattering mechanism.[15]

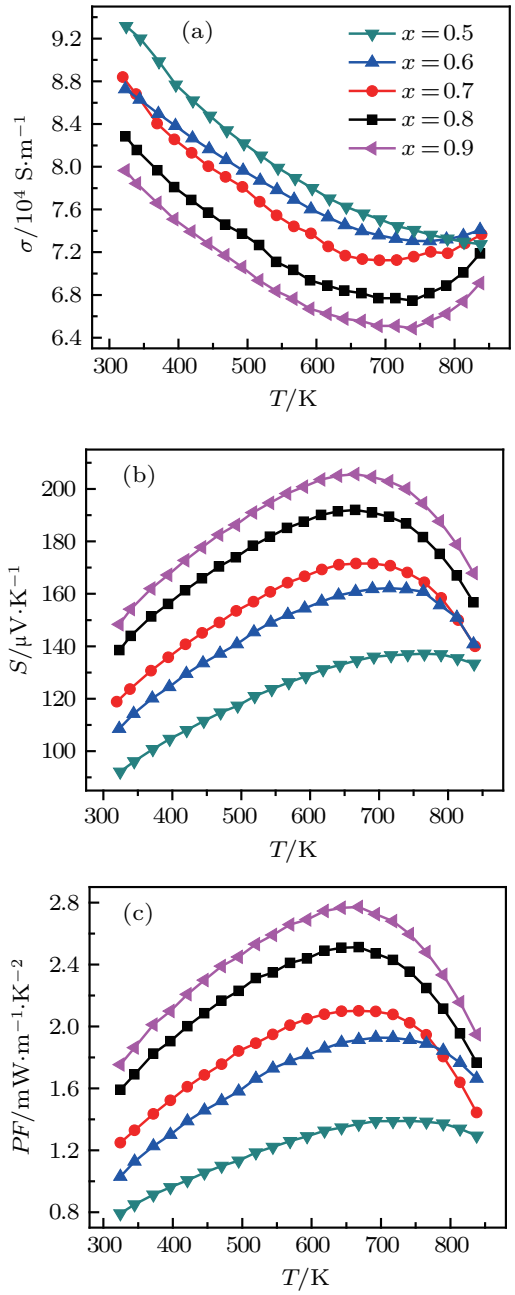


Fig. 3. (color online) Temperature-dependent electrical properties for $Nd_xFe_{3.2}Co_{0.8}Sb_{12}$ ($x = 0.5$, 0.6, 0.7, 0.8, and 0.9) samples, showing (a) electrical conductivities; (b) Seebeck coefficients, and (c) power factors.

Table 1. Room temperature transport properties of the $Nd_xFe_{3.2}Co_{0.8}Sb_{12}$ ($x = 0.5$, 0.6, 0.7, 0.8, and 0.9) skutterudites.

x	S/μV·K^{-1}	σ/10^4 S·m^{-1}	κ/W·m^{-1}·K^{-1}	PF/mW·m^{-1}·K^{-2}	p/10^{20} cm^{-3}	zT
0.5	104	9.31	2.15	0.85	5.50	0.11
0.6	124	8.72	2.11	1.12	4.80	0.15
0.7	135	8.83	1.89	1.32	4.10	0.21
0.8	156	8.82	1.93	1.68	3.90	0.26
0.9	167	7.96	2.02	1.86	3.50	0.28

Figure 3(b) shows the temperature dependence of the Seebeck coefficient (S) of $Nd_xFe_{3.2}Co_{0.8}Sb_{12}$ ($x = 0.5$, 0.6, 0.7, 0.8, and 0.9) filled skutterudites. The sample has a positive sign of Seebeck coefficient, which represents that the majority of charge carriers are holes. In the entire temperature range, the absolute value of the Seebeck coefficient first increases with increasing temperature, and then it starts to decrease due to the presence of an intrinsic semiconducting behavior at high temperature.[16] The Seebeck coefficient of p-type $Nd_xFe_{3.2}Co_{0.8}Sb_{12}$ is enhanced with increasing concentration of Nd, and the Seebeck coefficient for $Nd_{0.9}Fe_{3.2}Co_{0.8}Sb_{12}$ reaches a maximum value of 205 $\mu V \cdot K^{-1}$ at 670 K. Figure 3(c) demonstrates the temperature-dependent power factor (PF) of $Nd_xFe_{3.2}Co_{0.8}Sb_{12}$ ($x = 0.5$, 0.6, 0.7, 0.8, and 0.9) filled skutterudites. The maximum power factor reaches up to 2.7 $mW \cdot m^{-1} \cdot K^{-2}$ for the $Nd_{0.9}Fe_{3.2}Co_{0.8}Sb_{12}$ sample at 690 K, mainly resulting from the high Seebeck coefficient.

The temperature-dependent total thermal conductivities of $Nd_xFe_{3.2}Co_{0.8}Sb_{12}$ ($x = 0.5$, 0.6, 0.7, 0.8, and 0.9) filled skutterudites are shown in Fig. 4(a). The total thermal conductivity can be divided into the lattice thermal conductivity (κ_l) and the electronic thermal conductivity (κ_e), i.e., $\kappa = \kappa_l + \kappa_e$. The electronic component of the thermal conductivity (κ_e) is due to the heat transported by electrons while the lattice component of the thermal conductivity (κ_l) arises from the heat transported by the phonons. Here κ_e can be calculated from the Weidman–Franz law: $\kappa_e = L\sigma T$, where the Lorenz number is selected as the metallic limit value of 2.45×10^{-8} $V^2 \cdot K^{-2}$.[17] It is observed that the electrical thermal conductivity (κ_e) accounts for about 50% portion of the total thermal conductivity due to the high electrical conductivity. The calculated lattice thermal conductivities of all samples are displayed in Fig. 4(b). It is clearly seen that the thermal conductivity decreases after Nd filling because of the strong phonon scattering from the vibrational modes of the filling atoms. It is not surprising that the strategy of filling atoms is an effective way to reduce the lattice thermal conductivity, thereby greatly suppressing the total thermal conductivity. As a result, the lowest thermal conductivity is found to be 1.86 $W \cdot m^{-1} \cdot K^{-1}$ in $Nd_{0.7}Fe_{3.2}Co_{0.8}Sb_{12}$. Here the lattice thermal conductivities of all Nd-filled samples are less than 1.5 $W \cdot m^{-1} \cdot K^{-1}$ in a temperature range from room temperature to 650 K. In general, the filling fraction limitation is determined by the electronegativity, ionic radius and valance states. As is well known, the lattice thermal conductivity follows the T^{-1} relation when the Umkklap phonon scattering process dominates and decreases with the increasing filling fraction.[18] It cannot be ignored that the grain bounties and nanoparticles displayed in the SEM images still scatter phonons with the wavelengths ranging from the middle to long wavelength at high temperature. The lowest lattice thermal conductivity is found to be 0.89 $W \cdot m^{-1} \cdot K^{-1}$ at $x = 0.8$. The low lattice thermal conductivity can be mainly attributed to phonon–phonon scattering assisted with point defect Fe/Co with mass and strain fluctuation, boundary scattering particularly. However, the lattice thermal conductivity of $Nd_{0.9}Fe_{3.2}Co_{0.8}Sb_{12}$ increases suddenly due to the Sb impurity phase with high thermal conductivity. The phenomenon is common in other TE materials containing second phases, such as the SnO_2 impurity phase with high κ_l in SnSe polycrystal.[19]

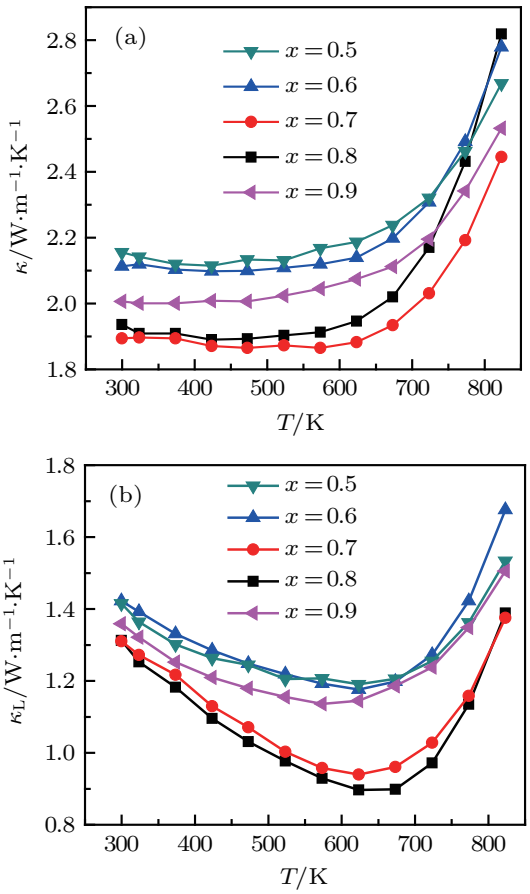


Fig. 4. (color online) Temperature-dependent thermal conductivities for $Nd_xFe_{3.2}Co_{0.8}Sb_{12}$ ($x = 0.5$, 0.6, 0.7, 0.8, and 0.9) samples, showing (a) thermal conductivities and (b) lattice thermal conductivities.

Figure 5 shows the temperature-dependent figure-of-merit (zT) calculated from the electrical conductivity, Seebeck coefficient, and thermal conductivity. The maximum zT value is found to be 0.87 in $Nd_{0.9}Fe_{3.2}Co_{0.8}Sb_{12}$ at 690 K as a result of the high power factor and low thermal conductivity as compared with those in other samples. The zT values of all samples increase with temperature and attain a maximum value in a temperature range of 665 K–690 K. As shown in Fig. 6, the zT value of our work is comparable to the previously reported values for the single filled skutterudites. Therefore, we conclude that the zT value of the p-type filled skutterudites could be improved through optimizing the carrier concentration and reducing the thermal conductivity by filling Nd and Fe for Co.

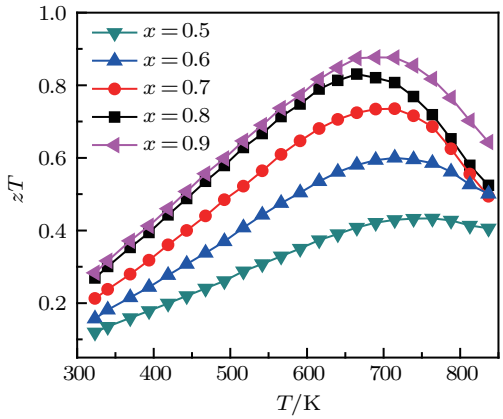


Fig. 5. (color online) Figure-of-merits for $Nd_xFe_{3.2}Co_{0.8}Sb_{12}$ ($x = 0.5$, 0.6, 0.7, 0.8, and 0.9) samples.

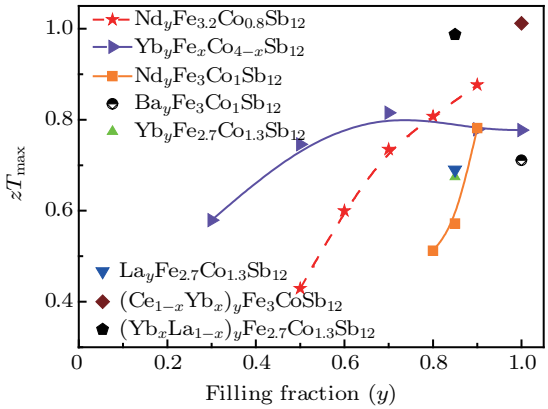


Fig. 6. (color online) Plots of the maximum zT versus the filling fraction for $Yb_yFe_xCo_{4-x}Sb_{12}$,[20] $Nd_yFe_3Co_1Sb_{12}$,[21] $Ba_yFe_3Co_1Sb_{12}$, $Yb_yFe_{2.7}Co_{1.3}Sb_{12}$, $La_yFe_{2.7}Co_{1.3}Sb_{12}$, $(Ce_{1-x}Yb_x)_yFe_3CoSb_{12}$,[22] $(Yb_xLa_{1-x})_yFe_{2.7}Co_{1.3}Sb_{12}$,[23] and this work ($Nd_yFe_{3.2}Co_{0.8}Sb_{12}$).

4. Conclusions

Nd-filled p-type skutterudites $Nd_xFe_{3.2}Co_{0.8}Sb_{12}$ ($x = 0.5$, 0.6, 0.7, 0.8, and 0.9) have been successfully synthesized by the solid-state reaction method, and their TE transport properties are investigated. Using Nd as a filler in skutterudites, the lowest value of lattice thermal conductivity, 0.89 $W{\cdot}m^{-1}{\cdot}K^{-1}$ at 630 K, is attained in the $Nd_{0.8}Fe_{3.2}Co_{0.8}Sb_{12}$ sample. The electrical conductivity of the samples decreases with increasing Nd concentration, which results from the diminished carrier concentration. A maximum zT value of 0.87 is achieved in $Nd_{0.9}Fe_{3.2}Co_{0.8}Sb_{12}$ at 690 K due to its high power factor and low thermal conductivity.

References

[1] Skutterudites Uher C 2001 *Prospective novel thermoelectrics. Semiconductors and semimetals* **69** 139
[2] Slack G A and Tsoukala V G 1994 *J. Appl. Phys.* **76** 1665
[3] Zhao L D, Dravid V P and Kanatzidis M G 2014 *Energy Environ. Sci.* **7** 251
[4] Sales B, Mandrus D and Williams R K 1996 *Science* **272** 1325
[5] Bell L E 2008 *Science* **321** 1457
[6] Morelli D T, Meisner G P, Chen B, Hu S and Uher C 1997 *Phys. Rev. B* **56** 7376
[7] Sales B, Mandrus D, Chakoumakos B, Keppens V and Thompson J 1997 *Phys. Rev. B* **56** 15081
[8] Rogl G, Grytsiv A, Bauer E, Rogl P and Zehetbauer M 2010 *Intermetallics* **18** 57
[9] Nordstr?m L and Singh D J 1996 *Phys. Rev. B* **53** 1103
[10] Tang X, Chen L, Goto T, Hirai T and Yuan R 2002 *J. Mater. Res.* **17** 2953
[11] Zhou C, Morelli D, Zhou X, Wang G and Uher C 2011 *Intermetallics* **19** 1390
[12] Tan G, Zheng Y and Tang X 2013 *Appl. Phys. Lett.* **103** 183904
[13] Zhou L, Qiu P, Uher C, Shi X and Chen L D 2013 *Intermetallics* **32** 209
[14] Chandra M R, Mueller E and Kim I H 2012 *J. Appl. Phys.* **111** 023708
[15] Duan B, Zhai P, Liu L, Zhang Q and Ruan X 2012 *J. Mater. Sci.: Materials in Electronics* **23** 1817
[16] Qiu P, Liu R, Yang J, Shi X, Huang X and Zhang W 2012 *J. Appl. Phys.* **111** 023705
[17] Xu C, Duan B, Ding S, Zhai P and Li P 2013 *Physica B: Conden. Matter* **425** 34
[18] Sales B, Mandrus D, Chakoumakos B, Keppens V and Thompson 1997 *Phys. Rev. B* **56** 15081
[19] Peng K L, Wu H, YanY C, Guo L J, Wang G Y, Lu X and Zhou X Y 2017 *J. Mater. Chem. A* **5** 14053
[20] Liu R H, Qiu P F, Chen X H, Huang X Y and Chen L D 2011 *J. Mater. Res.* **26** 1813
[21] Guo L J, Cai Z W, Xu X L, Peng K L, Wang G W, Wang G Y and Zhou X Y 2015 *J. Nanosci. Nanotechnol.* **5** 1
[22] Liu R H, Yang J, Chen X H, Shi X, Chen L D and Uher C 2011 *Intermetallics* **19** 1747
[23] Liu R H, Yang J, Chen X H, Shi X, Chen L D and Uher C 2013 *Intermetallics* **32** 209